J Nanostruct 10(2): 217-229, Spring 2020

RESEARCH PAPER

Adsorption of Gas Molecules on Graphene Doped with Mono and Dual Boron as Highly Sensitive Sensors and Catalysts

Salah Abdul Mahdi Khudair [1], *and Hamad Rahman Jappor* [2]*

[1] *Directorate of Education Babylon, Ministry of Education, Iraq*

[2] *Department of Physics, College of Education for Pure Sciences, University of Babylon, Iraq*

ARTICLE INFO

Article History:
Received 12 January 2020
Accepted 19 February 2020
Published 01 April 2020

Keywords:
Adsorption
Boron-doped graphene
DFT
Electronic properties
Gas sensor

ABSTRACT

First-principle calculations have been investigated to study the adsorption of the molecules (SO_2, CO, NH_3, CO_2, NO_2, and NO) on the surface of mono boron (B) B-doped and dual B-doped graphene sheets to explore their potential applications as sensors. Our findings indicate that the adsorption of (CO and NH_3) on B-doped graphene and (CO and SO_2) on dual B-doped graphene are weak physisorption with adsorption energy between (0.128 to 0.810) eV. However, the adsorption of (CO_2, NO_2, SO_2, and NO) on B-doped graphene and (CO_2, NH_3, NO and NO_2) on dual B-doped graphene are strong chemisorption. The strong interaction of (CO_2, NO_2, SO_2, and NO) on B-doped graphene and (CO_2, NH_3, NO and NO_2) on dual B-doped graphene demonstrating that B-doped graphene and dual B-doped graphene could catalyse or activate, suggesting the possibility of B-doped graphene and dual B-doped graphene as a catalyst. Moreover, the energy gap of B-doped graphene and dual B-doped graphene is opened upon adsorption of (CO, CO_2, NH_3, NO, NO_2 and SO_2) in various ways. Our calculations demonstrate the feasibility of B-doped graphene may be a good sensor for (CO and NH_3) and dual B-doped graphene could be a good sensor for (CO and SO_2).

How to cite this article
Khudair S. A. M. and Jappor H. R.. Adsorption of Gas Molecules on Graphene Doped with Mono and Dual Boron as Highly Sensitive Sensors and Catalysts. J Nanostruct, 2020; 10(2):217-229. DOI: 10.22052/JNS.2020.02.003

INTRODUCTION

The need for scale down sensors with fast response, high reliability, high sensitivity, high selectivity, low cost, and quick recovery has encouraged the scientists to try to find different gas sensing systems based on new nanomaterials. Graphene, the first discovered two-dimensional (2D) atomic crystal [1,2], Graphene represents a new material concept with only one atom thick, supplying scientists with another method to enter low-dimensional physics. By means of the research deepening, the manufacturing revolution carried by graphene will be immeasurable. Carbon is the versatile element on the crust of the earth and it is set up on the surface of the earth in dissimilar allotropes as diamonds, graphite, coke, and charcoal respectively. The newer allotropes of carbon were discovered such as graphene, carbon nanotubes (CNTs) and fullerenes [3–5]. Graphene is the youngest known allotrope of carbon, which is a two-dimensional and one-atom-thick material consisting of sp^2 hybridized carbon atoms organized in the structure of a honeycomb. These allotropes of carbon are extensively used in research, that is, from biomedical to environmental applications owing to their unique physical and chemical properties [6]. The exceptional properties of carbon and nanomaterials, such as electronic, thermal, optical, mechanical and transport properties make them encouraging candidates for various potential applications [7–11]. From several experimental and theoretical

* *Corresponding Author Email: hrjms@yahoo.com*

studies, it is observed that the transport and electronic properties are exceedingly sensitive to change in the local chemical environment [12–14], has attracted unlimited interest thanks to its astonishing properties, for example, high carrier mobility, high surface-volume ratio, high chemical stability, low electronic temperature noise, fast response time, and high thermal stability.

Ergo, it offers promise in the development of ultrasensitive gas sensors with high selectivity, fast recovery, high packing density, and low power consumption [15,16]. The applicability of graphene in the field of gas sensing has been widely investigated both experimentally [17,18]. and theoretically [19–24]. At present, there are three types of modification ways for the maximum conventional graphene, including electrostatic field tuning, chemical modification, and atomic doping [25–28]. Nowadays, the most feasible methods to control the semiconductor performance of graphene is the atomic doping which regarded as one of which can open the band gap of graphene, and significantly improve its electronic and optical properties [29–32]. It has been demonstrated that the graphene-based gas sensors sensitivity can be significantly improved by introducing dopants or defects [33–38]. Despite the great development and advances made in this field, there are still some restrictions in these nanomaterials, including but not limited to exposure to the mixture of gases, weak anti-interference faculty, delayed gas response, and low selectivity …. etc. Since the surface of nanomaterial doesn't only interact with one type of research gas, and most scientists only select the best from the adsorption outcomes to explain the selectivity of the surface of nanomaterial, while disregarding the interaction between other gas molecules and the surface of nanomaterial that has a very large influence on the adsorption results and they can't judge the type of adsorbed gas [39]. Owing to the effect of other gases, when the multi-adsorption happens, the academics can't differentiate which gas molecule has interacted with the surface of the material, so that the results can't be judged exactly. Consequently, it is very necessary to discover a sensing material capable of detecting the type of adsorbed gas molecules [40]. Boron atom is the most common candidate of p-type dopant for carbon materials. With the development of synthesis techniques, B-doped graphene has been fabricated [41]. In this work, first-principles methods depending on the density functional theory (DFT) are used to examine the electronic properties of the graphene after the interaction with toxic gas molecules such as NH3, SO_2, CO_2, NO_2, NO and CO. The sensitivity of the sensors is evaluated from the variations in their electronic transport properties. Our results reveal the promising future of graphene in the development of ultrahigh sensitive gas sensors [42].

COMPUTATIONAL METHODS AND MODELS

Computational Methods

All calculations are performed using DFT, the geometric structures were completely optimized using Gaussian 09 program package [43]. We chose the Perdew-Burke-Ernzerhof (PBE) exchange-correlation functional [44,45], to describe the exchange and correlation energy in the structural optimizations and total energy calculations. The system is modelled including 42 carbon atoms of B-doped graphene and dual B-doped graphene was created. The corresponding dopant concentration is 2.4% and 4.8% of B-doped graphene and dual B-doped graphene respectively. The adsorption energy (E_{ad}) of molecules on the B-doped graphene ($E_{ad\ (gas+\ B\text{-}doped\ graphene)}$) and dual B-doped graphene ($E_{ad\ (gas+\ dual\ B\text{-}doped\ graphene)}$) is defined as follows [46,47]:

$$E_{ad\ (gas+\ B\text{-}doped\ graphene)} = E_{(gas+\ B\text{-}doped\ graphene)} - (E_{B\text{-}doped\ graphene} + E_{gas}) \quad (1)$$

$$E_{ad\ (gas+\ dual\ B\text{-}doped\ graphene)} = E_{(gas+\ dual\ B\text{-}doped\ graphene)} - (E_{dual\ B\text{-}doped\ graphene} + E_{gas}) \quad (2)$$

where $E_{(gas+B\text{-}doped\ graphene)}$ and $E_{(gas+dual\ B\text{-}doped\ graphene)}$ are the total energies of the relaxed molecule on the B-doped graphene and dual B-doped graphene respectively, $E_{B\text{-}doped\ graphene}$ and $E_{dual\ B\text{-}doped\ graphene}$ are the energies of isolated B-doped graphene and dual B-doped graphene and E_{gas} is the energy of the isolated gas molecule. The diversity of relative energy of the highest occupied molecular orbital (E_{HOMO}) and the energy of lowest unoccupied molecular orbital (E_{LUMO}) of free B-doped graphene and dual B-doped graphene and adsorbed molecule on B-doped graphene and dual B-doped graphene gives the mechanism of interaction. The HOMO can be defined as an electron donor because of having an excess of electrons whereas the LUMO is lacking electrons and therefore it has a power of accepting electrons.

Computational Models

The graphene model was cut from optimized

graphite model. Graphene is a hexagonal monolayer atomic structure with a stable and symmetrical nature. The graphene molecular formula is C. Each one of carbon coordinates with other three atoms of carbon (arranged in a honeycomb polygon) and shapes a covalent molecule. The model of graphene as shown in Fig. 1 built using 3×3 supercell geometries. The lengths of C–C bonds are 1.42 Å [48], which is in agreement with the description of the literature [49].

RESULTS AND DISCUSSION

Electronic Structure of Doped Graphene

Graphene was doped with B and dual B atom, respectively, and the optimized models are shown in Fig. 2 (a) and (b). Doping graphene with other atoms or molecules is efficient ways to modify the structural and electronic properties of graphene. The doped atom is substituted with C atom. B-doped graphene and dual B-doped graphene retain the planar form of graphene after full relaxation and their corresponding model are given in Fig. 2 (a) and (b).

The free boron atom has an atomic configuration is $2s^2 2p^1$. When graphene is doped, the boron atom faultlessly binds with the three neighbouring carbon atoms and undergoes a sp^2 hybridization. Because of the dopant, the graphene a little deforms, the three B-C bonds for B-graphene are found to be 1.51 Å, while three B-C bonds for dual B-graphene is found to be 1.49 Å, which agrees with the theoretical results [50,51], which is increased than that of C-C bond length 1.42 Å in graphene, also note that the B_1-B_2 bond length for dual B-graphene is found to be 1.57 Å. All of those structural differences for B- and dual B-graphene could cause the variations of the electronic and structural properties [52]. However, the doping of boron atoms into graphene only results in a structural defect, it is not found unpaired electrons or distortion in the planar structure of the graphene sheet. Our results are in good agreement with the previous work that confirmed the planar structure of B-graphene [53].

Table 1 clarifies the effect of B-doped and dual B-doped on the electronic properties of graphene. The B-doped graphene has a large value of E_{HOMO}, and small values of E_{LUMO} and the Fermi energy (E_F) compared with dual B-doped graphene. As is clear table the Fermi energy (E_F) which is calculated from the E_{HOMO} and E_{LUMO} ($E_F = (E_{HOMO} + E_{LUMO})/2$) equal to -5.160 eV for B-doped graphene and -5.265 eV for dual B-doped graphene. The computed energy gap (E_g) for B-doped graphene is larger than dual B-doped graphene, however, the B-doped graphene and dual B-doped graphene are semiconductors with E_g equal to 1.307 eV and 0.172 eV, respectively.

It is clear that band gap is decreasing with increasing the concentrations of boron. The band gap decreasing upon doping is a well-known general phenomenon in semiconductors, not just in the present study. Shallow level donor impurities create energy levels in the band gap near the conduction band edge and shallow acceptor impurities create energy levels near the valence band edge. With the increase in the amount of boron concentration, the density of states of these dopants increases and forms a continuum of states just like in the bands and effectively the bandgap decreases. In other words, the system shows hole

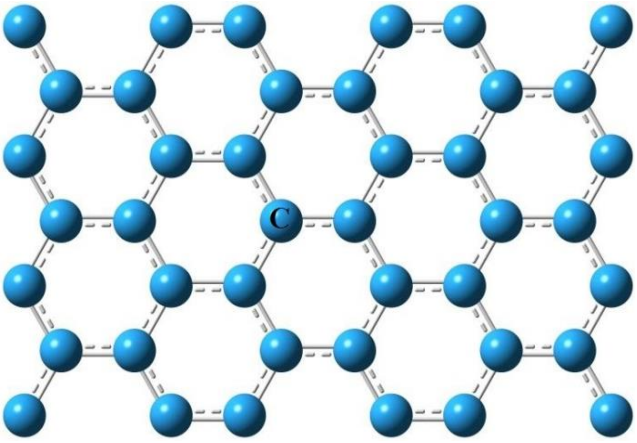

Fig. 1. The optimized structure of graphene in the present study.

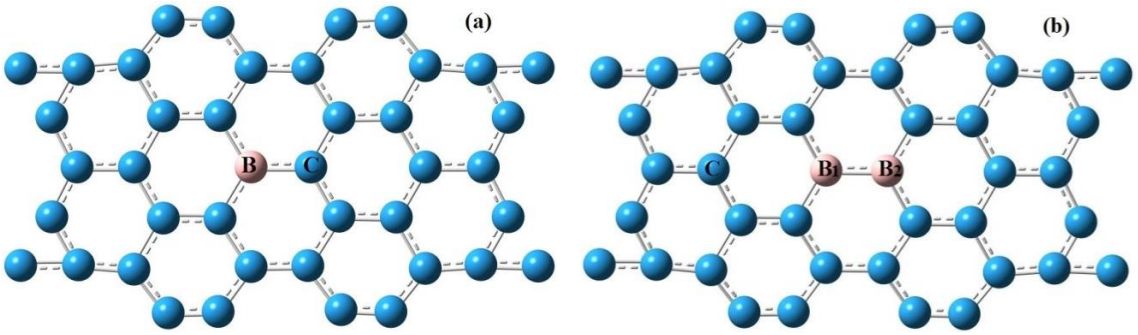

Fig. 2. The optimized structures of (a) boron- and (b) dual boron-doped graphene.

Table 1. The electronic properties of B- and dual B-graphene.

Property (eV)	B-graphene	dual B-graphene
E_g	1.307	0.172
E_{HOMO}	-5.813	-5.351
E_{LUMO}	-4.506	-5.179
E_F	-5.160	-5.265

doping properties because the boron is a p-type dopant, consequently causing transport in Dirac point overhead the Fermi energy. At the hole doping, most states are dragged overhead Fermi energy level, this leads to decrease in the band gap. Thus it is possible to alter the E_g of graphene sheet by doping B atom in the graphene sheet, as a result, this can affect the electronic properties of graphene [54,55].

There are various main peaks in the valence and conduction band, Fig. 3 (a) and (b) illustrates the DOS, the highest number of degenerate states in the conduction and valence bands is 5 for B-doped graphene and dual B-doped graphene. It is evident that there are states available for the occupation at high DOS for a specific energy level and no states can be occupied at a zero- DOS for energy level. Moreover, doping with dual B atom leads to a slight increase in the DOS in the conduction and valence bands in comparison with those of B-doped graphene as shown in Fig. 3.

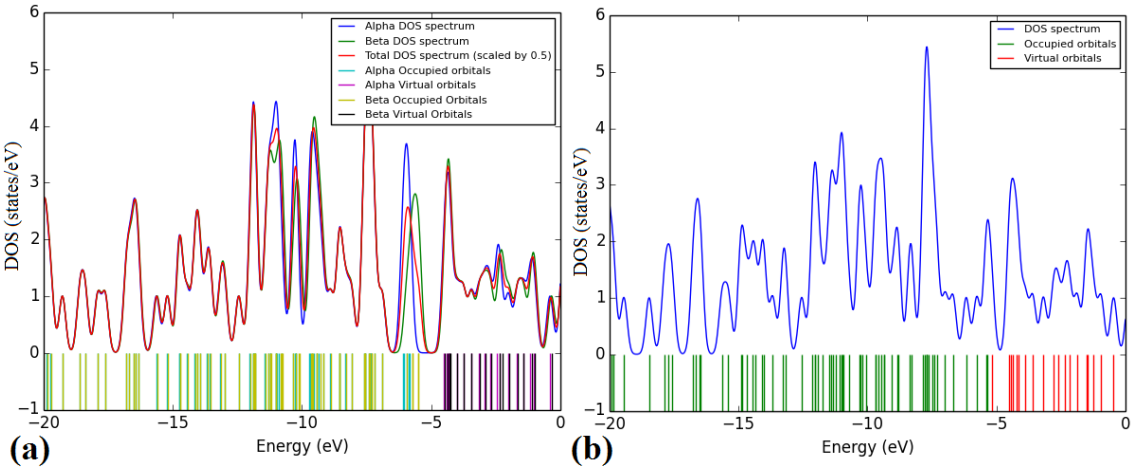

Fig. 3. The density of states (DOS) of (a) boron and (b) dual boron-doped graphene. Alpha DOS spectrum in the red line and beta DOS spectrum in the blue line.

Adsorption of Gas Molecules on Doped Graphene

The B- and dual B-graphene are studied to improve the interaction with the gaseous molecules. The boron has one less valence electron than carbon, therefore such type of doping will lead into a p-type semiconductor so hole is the main carrier, which indicates that the boron acts as an acceptor, and the gas molecules acts as a donor, this causes a large transfer of charge, and therefore a strong interaction between the electron-deficient B atom and the electron-donating atom of gas molecules, the reason that the gas molecules are adsorbed above the boron sites and not interacting with graphene carbons.

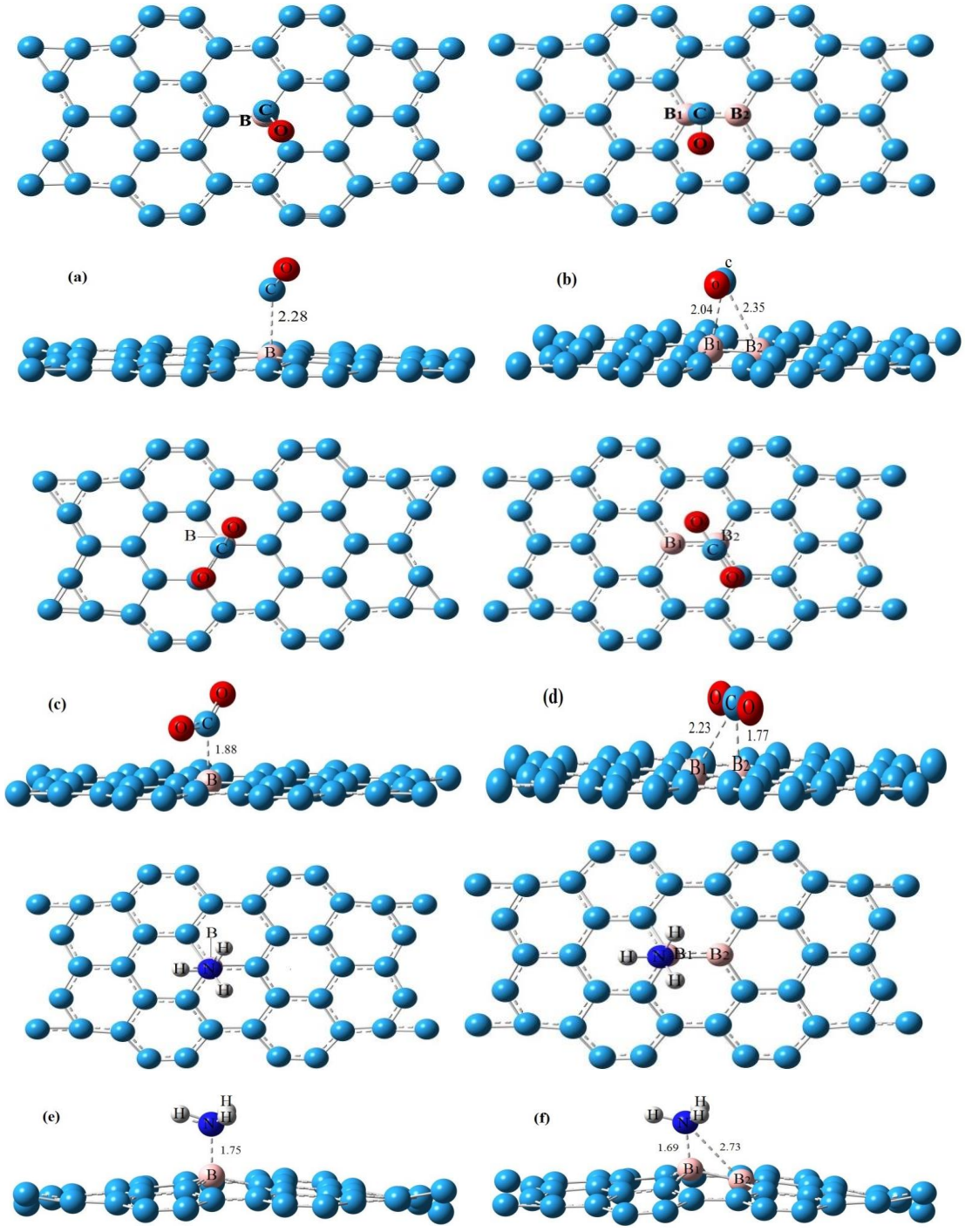

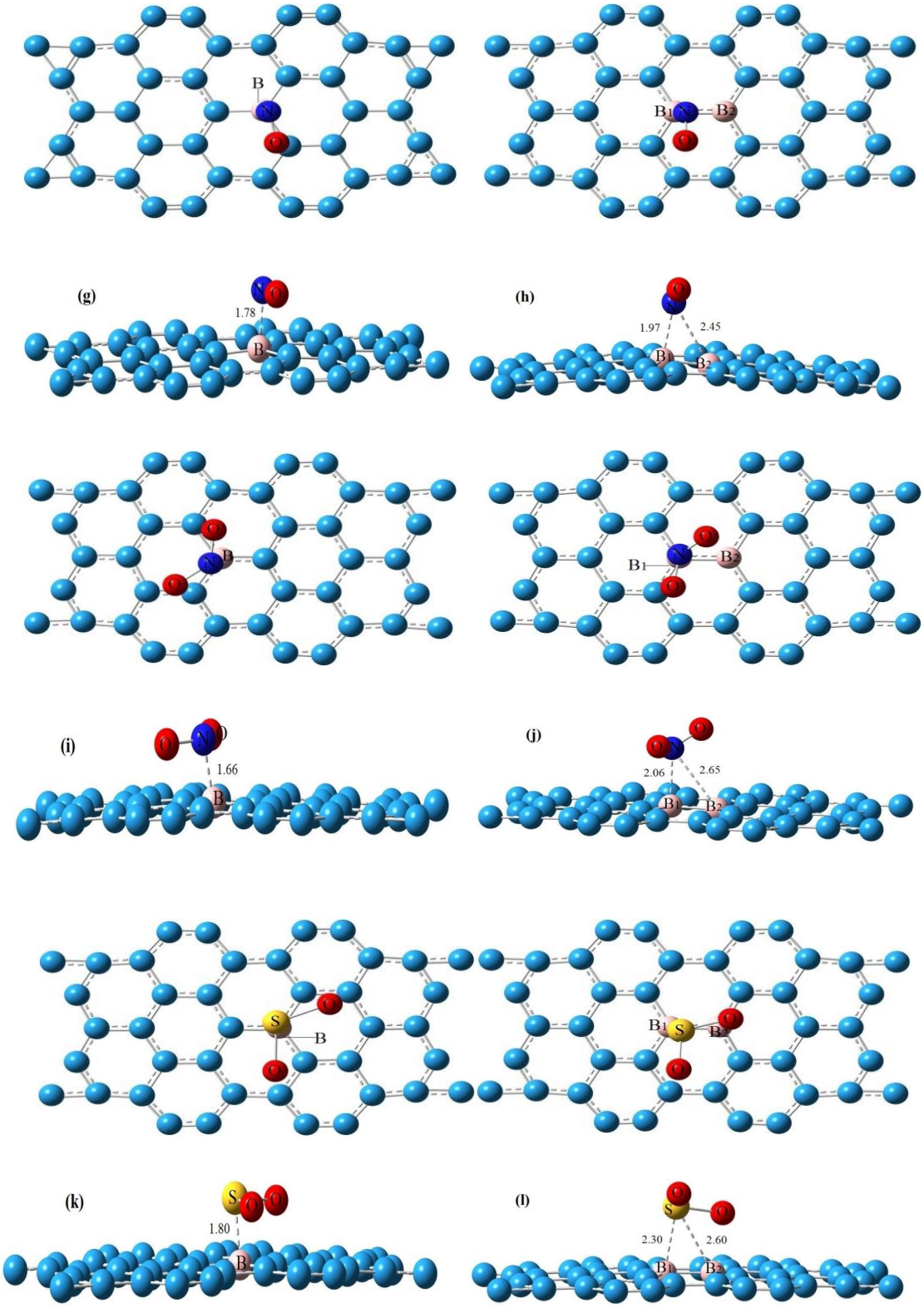

Fig. 4. Top and side views of the optimized structures of; adsorbed (a) CO, (c) CO_2, (e) NH_3, (g) NO, (i) NO_2 and (k) SO_2 gas molecules on boron-doped graphene, adsorbed (b) CO, (d) CO_2, (f) NH3, (h) NO, (j) NO_2 and (l) SO_2 gas molecules on dual boron-doped graphene.

We study the adsorption of CO, CO_2, NO, NO_2, NH_3 and SO_2 gases on B- and dual B-graphene near the dopant site. After adsorption of these gases, we try to examine its effect on structural, and electronic properties of B- and dual B-graphene. The optimized adsorption structure of CO adsorbed on B- and dual B-graphene is shown in Fig. 4(a) and (b), respectively. Meanwhile, we find that bond lengths of B-C, B_1-C and B_2-C are 2.28 Å, 2.04 Å and 2.35 Å, respectively, which is basically decreased with the increase of electrons in the elements, while the angles of B-C-O, B_1-C-O and B_2-C-O are 128°, 92° and 92°, respectively.

It can be noticed from Table 2, the E_g for adsorbed B-graphene is smaller than those of B-graphene, this point out that the E_g decreases with the adsorbed B-graphene, whereas the E_g for adsorbed dual B-graphene is larger than those of dual B-graphene, this indicates that E_g increases with the adsorbed dual B-graphene. The computed E_F for adsorption of CO on B-graphene is larger than the calculated value for B-graphene, whereas E_F for adsorption of CO on dual B-graphene is smaller than the calculated value for dual B-graphene. It has been found that the E_{HOMO} for adsorbed dual B-graphene is larger than the dual B-graphene and E_{LUMO} for adsorbed dual B-graphene is smaller than dual B-graphene, conversely, E_{HOMO} for adsorbed B-graphene is smaller than the B-graphene, while the E_{LUMO} for adsorbed B-graphene is larger than the B-graphene. The results show that the high value for E_{HOMO} is -5.813 eV, this value shows a propensity of the molecule to bestow electrons, whereas the lowest value of E_{LUMO} is -4.506 eV, this indicates a propensity of the molecule to accept electrons. The E_{ad} for adsorbed B-graphene and dual B-graphene are 0.81 eV and -0.503 eV corresponding to weak physisorption [56,57]. The binding strength of CO with B- and dual B-graphene are intermediate with the values of E_{ad}. Thus, B- and dual B-graphene can be successfully used to detect CO since the adsorption-desorption equilibrium of CO on B- and dual B-graphene are easily built.

Fig. 4(c) and (d) present that the most stable form of adsorbed CO_2 on B- and dual B-graphene, respectively. It has been found that bond lengths of B-C, B_1-C and B_2-C are 1.88Å, 2.23Å and 1.77Å, respectively, which basically decrease with the increase of electrons in the elements, meanwhile, the angles between the bonds B-C, B_1-C and B_2-C with the planes are 92°, 87° and 52° of B- and dual B-graphene, this is similar to the adsorption of CO on B- and dual B-graphene. Table 2 clarifies the effect of CO_2 adsorption on the electronic properties of B- and dual B-graphene. The results show that the E_g reduces with the adsorbed CO_2 on B- and dual B-graphene in comparison with B- and dual B-graphene. The adsorption of CO_2 on B- and dual B-graphene is larger than 1eV. Therefore, is a strong chemisorption, one can see from Table 2 that E_{HOMO} for adsorption of CO_2 on B-graphene is smaller than B-graphene, while E_{HOMO} for adsorbed dual B-graphene is larger than those of dual B-graphene. in return E_{LUMO} for adsorption of CO_2 on B- and dual B-graphene are larger than those of B- and dual B-graphene. The deduced results illustrate this larger value E_{HOMO} of adsorbed B-graphene is -5.813 eV, this value appears a propensity of the molecule to donate electrons and smaller value E_{LUMO} for B-graphene is -4.506 eV and display a propensity of the molecule to accepter electrons.

The NH_3 molecules are adsorbed to B- and dual B-graphene, via B atoms, as shown in Fig. 4(e) and (f). The bond lengths of B-N, B_1-N and B_2-N are 1.75 Å, 1.69 Å and 2.73 Å, respectively, basically decreases with the increase of electrons in the elements. Those values are consistent with the other for the length of bond B-N [53], while the angles between the bonds B-N, B_1-N and B_2-N with the planes of B- and dual B-graphene are 103°, 109° and 36°, respectively. The overall results of adsorbed NH_3 on B- and dual B-graphene are summarized in Table 2. The adsorption energies indicate that the tying strength of NH_3 with B-graphene is (-0.430 eV). Thus, B-graphene can be used to detect NH_3. Nevertheless, NH_3 on dual B-graphene could catalyse or activate this adsorbate due to the strong interaction, suggesting the possibility of dual B-graphene as catalyst. It is obvious from Tables 1 and 2 the adsorbed dual B-graphene lead to increase the E_g in comparison with dual B-graphene. The table shows the calculated E_{HOMO} and E_{LUMO} of adsorption of NH_3 on B- and dual B-graphene are smaller than those of B- and dual B-graphene.

The NO molecules are adsorbed to B- and dual B-graphene, via B atoms, as shown in Fig. 4(g) and (h). The bond lengths of B-N, B_1-N and B_2-N are 1.78 Å, 1.97 Å and 2.45 Å, respectively. The angles of B-N-O, B_1-N-O and B_2-N-O are 96°, 116° and 113°, respectively. The results indicate that E_{ad} for dual B-graphene is larger than B-graphene, in

Table 2. Electronic and Structural properties of different gases adsorbed on B- and dual B-graphene.

Device	Gas	E_{ad} (eV)	E_g (eV)	E_{HOMO} (eV)	E_{LUMO} (eV)	E_F (eV)
B-graphene	CO	0.810	1.084	-5.707	-4.623	-5.165
	CO_2	3.597	0.131	-4.841	-4.710	-4.776
	NH_3	-0.430	1.004	-5.213	-4.209	-4.711
	NO	3.347	0.066	-5.346	-5.280	-5.313
	NO_2	10.682	0.458	-5.278	-4.820	-5.049
	SO_2	7.146	0.517	-5.658	-5.141	-5.400
dual B-graphene	CO	-0.503	1.001	-5.658	-4.657	-5.158
	CO_2	-5.142	0.020	-5.608	-5.588	-5.598
	NH_3	-15.330	0.398	-5.139	-4.741	-4.940
	NO	-14.707	0.501	-5.785	-5.284	-5.535
	NO_2	7.746	0.853	-5.814	-4.961	-5.388
	SO_2	0.128	0.305	-5.694	-5.389	-5.542

the same way the E_g for adsorbed B-graphene is smaller than B-graphene, while the E_g for adsorbed dual B-graphene is larger than dual B-graphene, It can be seen that the E_{ad} for B- and dual B-graphene are a strong chemisorption, therefore, the B- and dual B-graphene are not suitable as a sensors of NO rather than B- and dual B-graphene can activate the adsorbate because of the strong interaction, proposing the possibility of B- and dual B-graphene as catalysts. Our results show that E_{HOMO} of adsorption of NO on B-graphene is smaller than B-graphene, while E_{HOMO} of adsorption of NO on dual B-graphene is larger than dual B-graphene, conversely, the E_{LUMO} of adsorption of NO on B- and dual B-graphene are larger than B- and dual B-graphene.

The NO_2 molecules are adsorbed to B- and dual B-graphene, via B atoms, as shown in Fig. 4(i) and (j). The optimized bond lengths of B-N, B_1-N and B_2-N are 1.66 Å, 2.06 Å and 2.65 Å. Those values are consistent with the other upshot for the length of bond B-N [24,58] at the same time that the angles between the bonds B-N, B_1-N and B_2-N with the planes of B- and dual B-graphene are 104°, 91° and 51°, respectively. Table 2 lists the results of adsorption of NO_2 on B- and dual B-graphene, it can be noticed that the E_g for adsorbed B-graphene smaller than those of B-graphene, conversely, the E_g for adsorbed dual B-graphene is greater than dual B-graphene. We found the adsorption of NO_2 on B- and dual B-graphene are a chemisorption for E_{ad} greater than 1eV, therefore, the B- and dual B-graphene are not suitable as a sensors of NO_2, rather than B- and dual B-graphene could activate this adsorbate, suggesting the possibility of B- and dual B-graphene as catalysts. The calculated E_{HOMO} of adsorption of NO_2 on B-graphene is smaller than B-graphene, while E_{HOMO} of adsorption of NO_2 on dual B-graphene is larger than dual B-graphene, conversely, the E_{LUMO} of adsorption of NO_2 on

B-graphene is larger than B-graphene, while E_{LUMO} of adsorption of NO_2 on dual B-graphene is smaller than dual B-graphene.

The SO_2 molecules are adsorbed to B- and dual B-graphene, via B atoms, as shown in Fig. 4(k) and (l). The bond lengths B-S, B_1-S and B_2-S are 1.80Å, 2.30Å and 2.60Å, respectively. While the angles between the bonds B-S, B_1-S and B_2-S with the planes of B- and dual B-graphene are 86°, 81° and 61°, respectively. If we discuss the adsorption of SO_2 on B- and dual B-graphene, we can deduce that E_g for adsorbed B-graphene is larger than adsorbed dual B-graphene, the E_{ad} for adsorbed dual B-graphene is smaller than adsorbed B-graphene, and E_F for adsorbed B-graphene is smaller than adsorbed dual B-graphene. Also, HOMO and LUMO energies for the adsorbed dual B-graphene is larger than dual B-graphene, conversely, E_{HOMO} of adsorption of SO_2 on B-graphene is smaller than B-graphene, while E_{LUMO} of adsorption of SO_2 on B-graphene is larger than B-graphene. One can see from the overall results that are displayed in Table 2, that the adsorbed SO_2 on dual B-graphene has a weakest adsorption of 0.128 eV with physisorption, indicating that dual B-graphene is sensitive to the gas SO_2. While the adsorbed SO_2 on B-graphene has the largest E_{ad} of 7.146eV that studied in the case of SO_2 adsorption with chemisorption. In other words, the B-graphene is not suitable as the sensor of SO_2. Instead of this, B-graphene can activate that adsorbate because of the strong interaction, proposing the probability of B-graphene as catalyst.

The density of states (DOS) of CO adsorption on B- and dual B-graphene illustrated in Fig. 5(a) and (b), respectively, the Figure shows that DOS of B- and dual B-graphene with the adsorption of gas molecules CO are different from the B- and dual B-graphene, the highest of peaks become less, i.e., the conduction and valence bands are less with the highest number of DOS. The showing DOS to the adsorption CO_2 on B- and dual B-graphene lead to decrease at DOS in the valence and conduction valence bands in comparison with DOS for B- and dual B-graphene, as depicted in Fig. 5(c) and (d), respectively. DOS to the adsorption NH_3 on B-graphene leads to decrease DOS in the valence and conduction bands in comparison with

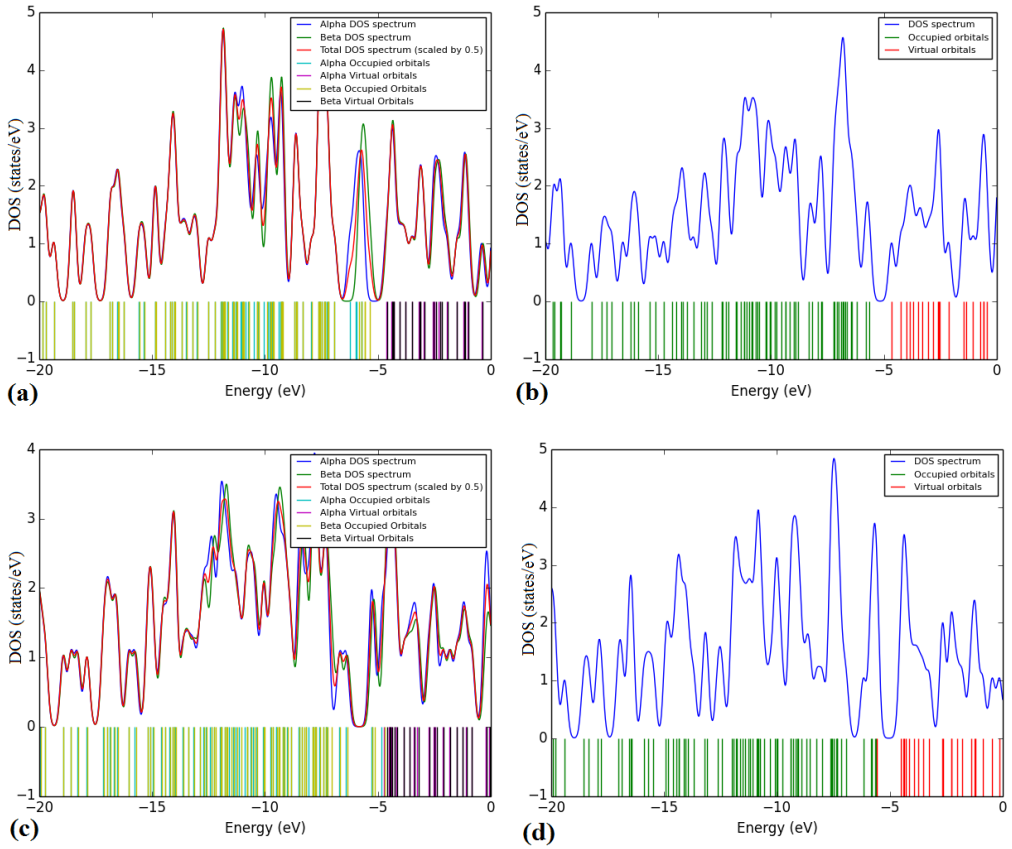

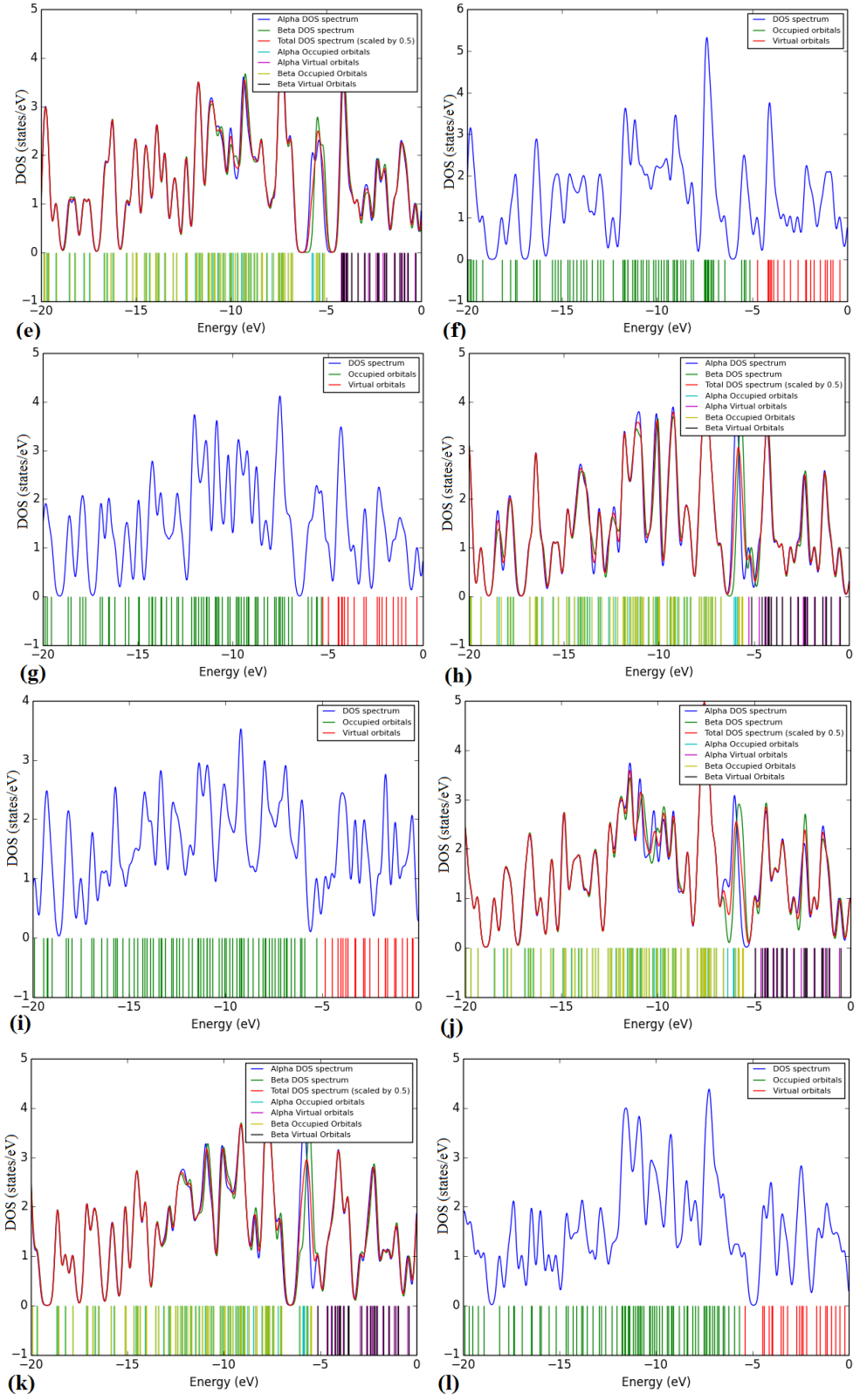

Fig. 5. DOS of adsorbed; (a) CO, (c) CO_2, (e) NH_3, (g) NO, (i) NO_2 and (k) SO_2 gas molecules on boron-doped graphene, (b) CO, (d) CO_2, (f) NH_3, (h) NO, (j) NO_2 and (l) SO_2 gas molecules on dual boron-doped graphene

DOS for B-graphene, whereas DOS for adsorption of NH_3 on dual B-graphene as function of energy levels shows that the adsorption of NH_3 on dual B-graphene is conformable with DOS of dual B-graphene, as depicted in Fig. 5(e) and (f), respectively. DOS for adsorption of NO on B- and dual B-graphene lead to a decrease in DOS in the conduction and valence bands in comparison with DOS of B- and dual B-graphene, as depicted in Fig. 5(g) and (h), respectively. On the other hand, DOS for adsorption of NO_2 molecules on B- and dual B-graphene revealed that DOS decrease in comparison with DOS of B- and dual B-graphene, see Fig. 5(i) and (j), respectively.

Finally, DOS for adsorption of SO_2 on B- and dual B-graphene in Fig. 5(k) and (l) illustrate that SO_2 adsorbed gas molecules adsorbed cause a decrease in the maximum number of DOS in the valence and conduction bands, in comparison with B- and dual B-graphene.

CONCLUSION

First-principles calculations have been performed to investigate the effect of adsorbed CO, CO_2, NH_3, NO, NO_2 and SO_2 molecules on the electronic properties of boron-doped graphene and dual boron-doped graphene surfaces. It can be deduced from our outcomes that the CO and NH_3 adsorbed gas molecules on B-doped graphene is accomplished by physisorption interaction with moderate adsorption energy. Simultaneously, the of CO_2, NO, NO_2 and SO_2 adsorption molecules on B-doped graphene are strong chemisorptions with higher adsorption energy. Furthermore, the B-doped graphene is strongly reactive with CO_2, NO, NO_2 and SO_2 adsorbed gas molecules, because these gases slow desorption from B-doped graphene. Consequently, B-doped graphene is not practicable as a gas sensor for these molecules. On the other hand, the B-doped graphene can be used as a catalyst. Besides, our conjecture that B-doped graphene is adequate to sensitively monitor CO and NH_3 sensors with moderate adsorption energy. However, the adsorption of gas molecules CO_2, NH_3, NO and NO_2 on dual B-doped graphene undergo in a strong chemisorption interaction, so it presumably unsuitable for usage as a gas sensor for these gases. In the same time, the adsorptions of CO and SO_2 on dual B-doped graphene are a weak physisorption with E_{ad} ranging from 0.128 eV to -0.503 eV. Hence, it can be used as a good sensor for CO and SO_2. It has been demonstrated that most of the adsorption energies are positive corresponds to the endothermic reaction, except that the adsorption of NH_3 on B-doped graphene and the adsorption of CO, CO_2, NH_3, NO on dual B-doped graphene are negative corresponds to the exothermic reaction. Our results reveal that the electronic properties of graphene can be stirringly modulated by boron doping and molecules adsorption, which could be used to design chemical sensors and graphene, could be used to build sensors for the detection of particular molecules.

CONFLICT OF INTEREST

The authors declare that there is no conflict of interests regarding the publication of this manuscript.

REFERENCES

1. Novoselov KS, Geim AK, Morozov SV, Jiang D, Zhang Y, Dubonos SV, Firsov AA, Grigorieva VI. Electric Field Effect in Atomically Thin Carbon Films. Science (80-) 2004;306:666–669.
2. Novoselov KS, Fal VI, Colombo L, Gellert PR, Schwab MG, Kim K. A roadmap for graphene. Nature 2012;490:192.
3. Hirsch A. The era of carbon allotropes. Nat Mater 2010;9:868–871.
4. Rao CNR, Sood AK, Subrahmanyam KS, Govindaraj A. Graphene: The New Two-Dimensional Nanomaterial. Angew Chemie Int Ed 2009;48:7752–7777.
5. Iijima S. Helical microtubules of graphitic carbon. Nature 1991;354:56–58.
6. Liu J, Cui L, Losic D. Graphene and graphene oxide as new nanocarriers for drug delivery applications. Acta Biomater 2013;9:9243–9257.
7. Hoat DM, Vu TV., Obeid MM, Jappor HR. Assessing optoelectronic properties of PbI_2 monolayer under uniaxial strain from first principles calculations. Superlattices Microstruct 2019;130:354–360.
8. Jappor HR, Habeeb MA. Tunable electronic and optical properties of GaS/GaSe van der Waals heterostructure. Curr Appl Phys 2018;18:673–680.
9. Jappor HR, Obeid MM, Vu TV., Hoat DM, Bui HD, Hieu NN, Edrees SJ, Mogulkoc Y, Khenata Y. Engineering the optical and electronic properties of Janus monolayer Ga_2SSe by biaxial strain. Superlattices Microstruct 2019;130:545–553.
10. Abed Al- Abbas SS, Muhsin MK, Jappor HR. Tunable optical and electronic properties of gallium telluride monolayer for photovoltaic absorbers and ultraviolet detectors. Chem Phys Lett 2018;713:46–51.
11. Bui HD, Jappor HR, Hieu NN. Tunable optical and electronic properties of Janus monolayers Ga_2SSe, Ga_2STe, and Ga_2SeTe as promising candidates for ultraviolet photodetectors applications. Superlattices Microstruct 2019;125:1–7.
12. Abed Al-Abbas SS, Muhsin MK, Jappor HR. Two-dimensional GaTe monolayer as a potential gas sensor for SO_2 and NO_2 with discriminate optical properties.

Superlattices Microstruct 2019;135:106245.
13. Zhong J, Chiou J, Dong C, Glans P-A, Pong W-F, Chang C, Wu Z, Guo J. Interfacial interaction of gas molecules and single-walled carbon nanotubes. Appl Phys Lett 2012;100:201605.
14 Zhao L, Chang H, Zhao W, Luan Z, Tian X, Tan C, Huang Y. Coexistence of doping and strain to tune electronic and optical properties of GaN monolayer. Superlattices Microstruct 2019;130:93–102.
15. He Q, Wu S, Yin Z, Zhang H. Graphene-based electronic sensors. Chem Sci 2012;3:1764.
16. Basu S, Bhattacharyya P. Recent developments on graphene and graphene oxide based solid state gas sensors. Sensors Actuators B Chem 2012;173:1–21.
17. Fowler JD, Allen MJ, Tung VC, Yang Y, Kaner RB, Weiller BH. Practical Chemical Sensors from Chemically Derived Graphene. ACS Nano 2009;3:301–306.
18. Ko G, Kim H-Y, Ahn J, Park Y-M, Lee K-Y, Kim J. Graphene-based nitrogen dioxide gas sensors. Curr Appl Phys 2010;10:1002–1004.
19. Jappor HR, Khudair SAM. Electronic properties of adsorption of CO, CO_2, NH_3, NO, NO_2 and SO_2 on nitrogen doped graphene for gas sensor applications. Sens Lett 2017;15:432–439.
20. Jappor HR, Khudair SAM. Al-Doped Graphene as a Sensor for Harmful Gases (CO, CO_2, NH_3 , NO, NO_2 and SO_2). Sens Lett 2017;15:1023–1030.
21. Jappor HR, Jaber AS. Electronic properties of CO and CO_2 adsorbed silicene/graphene nanoribbons as a promising candidate for a metal-free catalyst and a gas sensor. Sens Lett 2016;14:989–995.
22. Jappor HR. Electronic and structural properties of gas adsorbed graphene-silicene hybrid as a gas sensor. J Nanoelectron Optoelectron 2017;12:742–747.
23. Liang X-Y, Ding N, Ng S-P, Wu C-ML. Adsorption of gas molecules on Ga-doped graphene and effect of applied electric field: A DFT study. Appl Surf Sci 2017;411:11–17.
24. Dai J, Yuan J, Giannozzi P. Gas adsorption on graphene doped with B, N, Al, and S: A theoretical study. Appl Phys Lett 2009;95:232105.
25. Geim AK, Novoselov KS. The rise of graphene. Nat Mater 2007;6:183–191.
26. Schiros T, Nordlund D, Palova L, Zhao L, Levendorf M, Jaye C, Reichman D, Park J, Hybertsen M, Pasupathy A. Atomistic Interrogation of B–N Co-dopant Structures and Their Electronic Effects in Graphene. ACS Nano 2016;10:6574–6584.
27. Castro EV., Novoselov KS, Morozov SV., Peres NMR, dos Santos JMBL, Nilsson J, Guinea F, Geim AK, Neto AHC. Biased Bilayer Graphene: Semiconductor with a Gap Tunable by the Electric Field Effect. Phys Rev Lett 2007;99:216802.
28. Yavari F, Kritzinger C, Gaire C, Song L, Gulapalli H, Borca-Tasciuc T, Ajayan PM, Koratkar N. Tunable Bandgap in Graphene by the Controlled Adsorption of Water Molecules. Small 2010;6:2535–2538.
29. Janaszek B, Tyszka-Zawadzka A, Szczepański P. Tunable graphene-based hyperbolic metamaterial operating in SCLU telecom bands. Opt Express 2016;24:24129.
30. Wu Z-S, Ren W, Xu L, Li F, Cheng H-M. Doped Graphene Sheets As Anode Materials with Superhigh Rate and Large Capacity for Lithium Ion Batteries. ACS Nano 2011;5:5463–5471.
31. Rani P, Dubey GS, Jindal VK. DFT study of optical properties of pure and doped graphene. Phys E Low-Dimensional Syst Nanostructures 2014;62:28–35.
32. Kumar NA, Baek J-B. Doped graphene supercapacitors. Nanotechnology 2015;26:492001.
33. Rad AS. First principles study of Al-doped graphene as nanostructure adsorbent for NO_2 and N_2O: DFT calculations. Appl Surf Sci 2015;357:1217–1224.
34. Wanno B, Tabtimsai C. A DFT investigation of CO adsorption on VIIIB transition metal-doped graphene sheets. Superlattices Microstruct 2014;67:110–117.
35. Najafi M. DFT Study of Cyanide Oxidation on Ge-Doped Carbon Nanotubes. Russ J Appl Chem 2017;90:1620–1626.
36. Nasehnia F, Seifi M. Adsorption of molecular oxygen on VIIIB transition metal-doped graphene: A DFT study. Mod Phys Lett B 2014;28:1450237.
37. Dai J, Yuan J. Adsorption of molecular oxygen on doped graphene: Atomic, electronic, and magnetic properties. Phys Rev B 2010;81:165414.
38. Guo Y, Chen Z, Wu W, Liu Y, Zhou Z. Adsorption of NO_x (x = 1, 2) gas molecule on pristine and B atom embedded γ-graphyne based on first-principles study. Appl Surf Sci 2018;455:484–491.
39. Cortés-Arriagada D, Villegas-Escobar N, Ortega DE. Fe-doped graphene nanosheet as an adsorption platform of harmful gas molecules (CO, CO_2, SO_2 and H_2S), and the co-adsorption in O_2 environments. Appl Surf Sci 2018;427:227–236.
40. Gao C, Zhang Y, Yang H, Liu Y, Liu Y, Du J, Ye H, Zhang G. A DFT study of In doped Tl_2O: a superior NO_2 gas sensor with selective adsorption and distinct optical response. Appl Surf Sci 2019;494:162–169.
41. Palnitkar UA, Kashid R V., More MA, Joag DS, Panchakarla LS, Rao CNR. Remarkably low turn-on field emission in undoped, nitrogen-doped, and boron-doped graphene. Appl Phys Lett 2010;97:063102.
42. Duan K, Li L, Hu Y, Wang X. Pillared graphene as an ultra-high sensitivity mass sensor. Sci Rep 2017;7:14012.
43. Frisch, M.J., Trucks, G.W., Schlegel, H.B., Scuseria, G.E., Robb, M.A., Cheeseman, J.R., Scalmani, G., Barone, V., Mennucci, B., Petersson, G.A., Nakatsuji, H., Caricato, M., Li, X., Hratchian, H.P., Izmaylov, A.F., Bloino, J., Zheng, G., Sonnenberg, J.L., Hada, M., Ehara, M., Toyota, K., Fukuda, R., Hasegawa, J., Ishida, M., Nakajima, T., Honda, Y., Kitao, O., Nakai, H., Vreven, T., Montgomery Jr., J.A., Peralta, J.E., Ogliaro, F., Bearpark, M., Heyd, J.J., Brothers, E., Kudin, K.N., Staroverov, V.N., Kobayashi, R., Normand, J., Raghavachari, K., Rendell, A., Burant, J.C., Iyengar, S.S., Tomasi, J., Cossi, M., Rega, N., Millam, J.M., Klene, M., Knox, J.E., Cross, J.B., Bakken, V., Adamo, C., Jaramillo, J., Gomperts, R., Stratmann, R.E., Yazyev, O., Austin, A.J., Cammi, R., Pomelli, C., Ochterski, J.W., Martin, R.L., Morokuma, K., Zakrzewski, V.G., Voth, G.A., Salvador, P., Dannenberg, J.J., Dapprich, S., Daniels, A.D., Farkas, O., Foresman, J.B., Ortiz, J.V., Cioslowski, J. and Fox, D.J. (2010) Gaussian 09, Revision B.01. Gaussian Inc., Wallingford.
44. Perdew JP, Burke K, Ernzerhof M. Generalized Gradient Approximation Made Simple. Phys Rev Lett 1996;77:3865–3868.
45. Obeid MM, Jappor HR, Edrees SJ, Shukur MM, Khenata R, Mogulkoc Y. The electronic, half-metallic, and magnetic properties of $Ca_{1-x}Cr_xS$ ternary alloys: Insights from the first-principle calculations. J Mol Graph Model 2019;89:22–32.

46. Jappor HR. Band-structure calculations of GaAs within semiempirical large unit cell method. Eur J Sci Res 2011;59:264–275.
47. Jappor HR, Saleh ZA, Abdulsattar MA. Simulation of Electronic Structure of Aluminum Phosphide Nanocrystals Using Ab Initio Large Unit Cell Method. Adv Mater Sci Eng 2012;2012:1–6.
48. Heyrovska R. Atomic Structures of Graphene, Benzene and Methane with Bond Lengths as Sums of the Single, Double and Resonance Bond Radii of Carbon 2008.
49. Abergel DSL, Pietiläinen P, Chakraborty T. Electronic compressibility of graphene: The case of vanishing electron correlations and the role of chirality. Phys Rev B 2009;80:081408.
50. Jung SC, Kang Y-J, Yoo D-J, Choi JW, Han Y-K. Flexible Few-Layered Graphene for the Ultrafast Rechargeable Aluminum-Ion Battery. J Phys Chem C 2016;120:13384–13389.
51. Zhou YG, Zu XT, Gao F, Nie JL, Xiao HY. Adsorption of hydrogen on boron-doped graphene: A first-principles prediction. J Appl Phys 2009;105:014309.
52. Lee S-M, Kim J-H, Ahn J-H. Graphene as a flexible electronic material: mechanical limitations by defect formation and efforts to overcome. Mater Today 2015;18:336–44.
53. Bi DM, Qiao L, Hu XY, Zhi W. Theoretical Investigation of the Adsorption of NH_3 on B-Doped Graphene. Key Eng Mater 2011;474–476:720–724.
54. Saha M, Ghosh S, Ashok VD, De SK. Carrier concentration dependent optical and electrical properties of Ga doped ZnO hexagonal nanocrystals. Phys Chem Chem Phys 2015;17:16067–16079.
55. Yang N, Yang D, Chen L, Liu D, Cai M, Fan X. Design and adjustment of the graphene work function via size, modification, defects, and doping: a first-principle theory study. Nanoscale Res Lett 2017;12:642.
56. Feng J, Liu Y, Wang H, Zhao J, Cai Q, Wang X. Gas adsorption on silicene: A theoretical study. Comput Mater Sci 2014;87:218–226.
57. Hu PA, Wang L, Yoon M, Zhang J, Feng W, Wang X, Wen Z, Idrobo JC, Miyamoto Y., Geohegan DB, Xiao K. Highly Responsive Ultrathin GaS Nanosheet Photodetectors on Rigid and Flexible Substrates. Nano Lett 2013;13:1649–1654.
58. Choudhuri I, Patra N, Mahata A, Ahuja R, Pathak B. B–N@ Graphene: Highly Sensitive and Selective Gas Sensor. J Phys Chem C 2015;119:24827–24836.